ACADEMIC PRESS

Available online at www.sciencedirect.com

SCIENCE DIRECT®

Developmental Biology 262 (2003) 225–241

DEVELOPMENTAL BIOLOGY

www.elsevier.com/locate/ydbio

Cortical and retinal defects caused by dosage-dependent reductions in VEGF-A paracrine signaling☆

Jody J. Haigh,[a] Paula I. Morelli,[b] Holger Gerhardt,[b] Katharina Haigh,[a] John Tsien,[a] Annette Damert,[a,1] Lucile Miquerol,[a,2] Ulrich Muhlner,[c] Rudiger Klein,[d] Napoleone Ferrara,[e] Erwin F. Wagner,[c] Christer Betsholtz,[b] and Andras Nagy[a,*]

[a] *Mount Sinai Hospital, Samuel Lunenfeld Research Institute, Toronto, Canada*
[b] *Department of Medical Biochemistry, University of Gothenburg, Gothenburg, Sweden*
[c] *Research Institute for Molecular Pathology (IMP), Vienna, Austria*
[d] *Max-Plank Institute of Neurobiology, Martinsried, Germany*
[e] *Department of Molecular Oncology, Genentech, San Francisco, CA, USA*

Received for publication 12 March 2003, revised 28 May 2003, accepted 30 May 2003

Abstract

To determine the function of VEGF-A in nervous system development, we have utilized the Nestin promoter-driven Cre recombinase transgene, in conjunction with a conditional and hypomorphic VEGF-A allele, to lower VEGF-A activity in neural progenitor cells. Mice with intermediate levels of VEGF-A activity showed decreased blood vessel branching and density in the cortex and retina, resulting in a thinner retina and aberrant structural organization of the cortex. Severe reductions in VEGF-A led to decreases in vascularity and subsequent hypoxia, resulting in the specific degeneration of the cerebral cortex and neonatal lethality. Decreased neuronal proliferation and hypoxia was evident at E11.5, leading to increased neuronal apoptosis in the cortex by E15.5. In order to address whether the observed changes in the structural organization of the nervous system were due to a direct and autocrine role of VEGF-A on the neural population, we conditionally inactivated the main VEGF-A receptor, Flk1, specifically in neuronal lineages, by using the Nestin Cre transgene. The normality of these mice ruled out the possibility that VEGF-A/Flk1 signaling has a significant autocrine role in CNS development. VEGF-A dosage is therefore a critical parameter regulating the density of the vascular plexus in the developing CNS that is in turn a key determinant in the development and architectural organization of the nervous system.

Keywords: VEGF-A; Cre recombinase; Conditional gene inactivation; Blood vessel; Endothelium; Nervous system; Cortex; Retina

Introduction

Vascular Endothelial Growth Factor-A (VEGF-A) and its receptors (VEGFR1/Flt1, VEGFR2/Flk1, and Neuropilin-1) have been demonstrated to play pivotal roles in blood vessel development. The lethality of embryos heterozygous for a targeted null allele of VEGF-A (VEGF-$A^{null/+}$) (Carmeliet et al., 1996; Ferrara et al., 1996) and the lethality associated with the twofold overexpression (Miquerol et al., 2000) of this growth factor clearly demonstrate that only a narrow window of VEGF-A expression levels are compatible with the normal development of the cardiovascular system. The embryonic lethal phenotypes associated with the deficiencies in VEGF-A receptors further underscore the essential nature of VEGF-A-induced signaling (Fong et al., 1995; Kawasaki et al., 1999; Shalaby et al., 1995). The most severe endothelial defects were documented in Flk1 null embryos with lethality around embryonic stage 8.5 (E8.5) as a result of a complete failure of endothelial, hematopoietic, and endocardial differentiation (Shalaby et al., 1995).

☆ Supplementary data associated with this article can be found at doi: 10.1016/S0012-1606(03)00356-7.

* Corresponding author. Fax: +416-586-8588.
E-mail address: nagy@mshri.on.ca (A. Nagy).
[1] Present address: Paul-Ehrlich-Institute, Langen, Germany.
[2] Present address: IBDM-LGPD campus de Luminy, Marseille, France.

0012-1606/$ – see front matter © 2003 Elsevier Inc. All rights reserved.
doi:10.1016/S0012-1606(03)00356-7

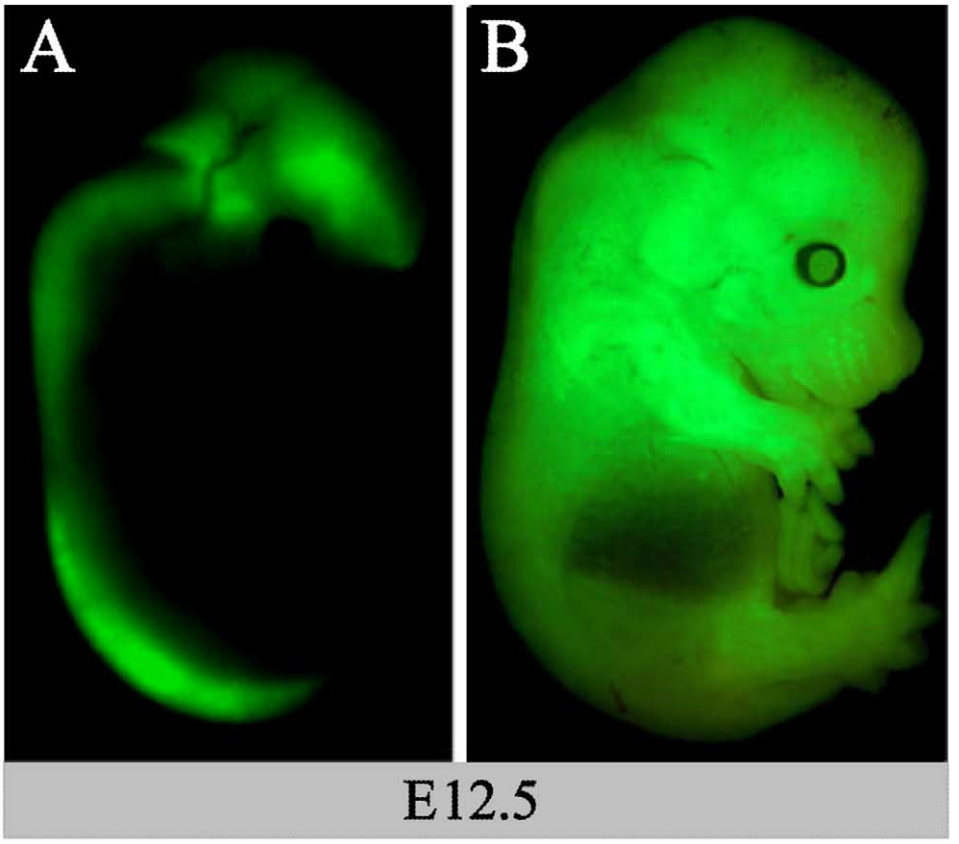
A
B
E12.5

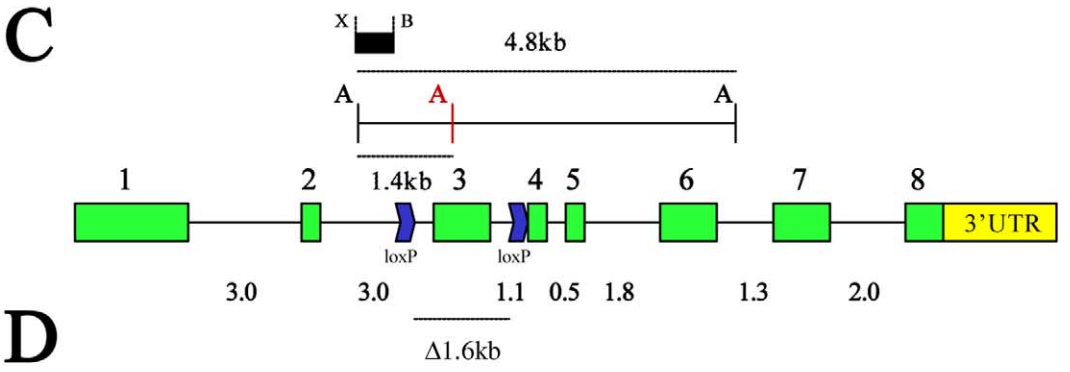
C
X
B
4.8kb
A
A
A
1
2
1.4kb
3
4
5
6
7
8
3'UTR
loxP
loxP
3.0
3.0
1.1
0.5
1.8
1.3
2.0
Δ1.6kb

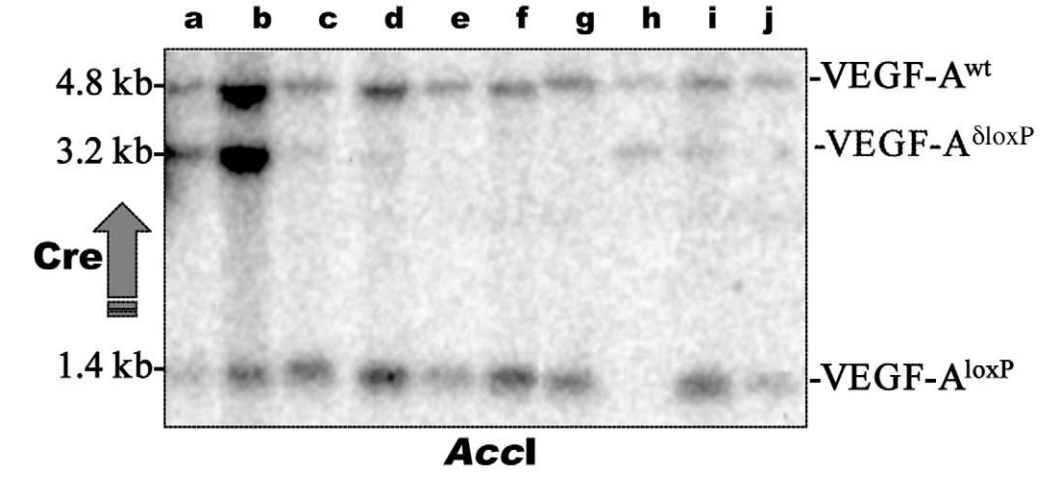
D
a
b
c
d
e
f
g
h
i
j
4.8 kb
3.2 kb
Cre
1.4 kb
-VEGF-A^wt
-VEGF-A^δloxP
-VEGF-A^loxP
AccI

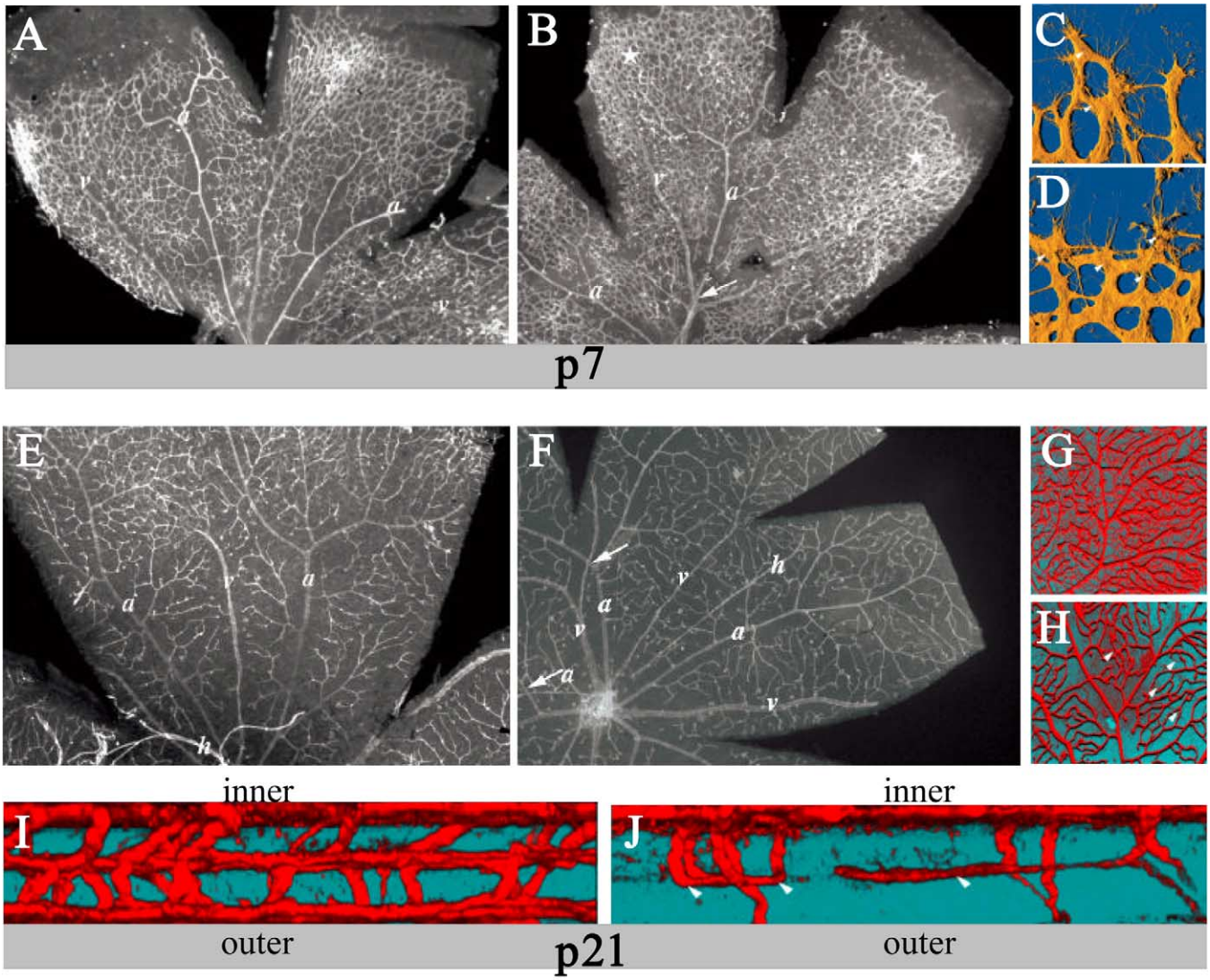

Fig. 2. Vascularization of the retina visualized by flat-mount, isolectin-B4 immunofluorescence staining. (A) Wild type P7 retina shows regular alternating pattern of arteries (a) and veins (v). Asterisk denotes developing vascular plexus. (B) Same stage VEGF-A$^{nescre/+}$ retina shows increased density of more immature vessels (asterisk). (C, D) 3-D illustration of sprouting tips of remodeling endothelial cells in both wild type and VEGF-A$^{nescre/+}$ P7 retinas, respectively. In both, the tip cells extend long filopodia towards the periphery. However, ectopic filopodia with irregular orientations seem to be more prominent in mutants (E) Wild type retina at P21 shows normal vessel remodeling and alternating patterns of arteries (a), veins (v), and hyaloid vessel (h). (F) P21 VEGF$^{nescre/+}$ retina lacks the outer capillary plexus with arteries and veins frequently crossing over in the inner vascular plexus (white arrows). 3-D reconstruction of the wild type (G) and VEGF-A$^{nescre/+}$ (H) retinal capillary vasculature at P21, respectively. In the wild type retina, larger vessels are visible in the uppermost vascular layer (retinal fiber layer) viewed from above. A dense capillary plexus develops both in the inner and outer plexiform layer. The VEGF-A$^{nescre/+}$ retina frequently lacks large parts of the outer retinal plexuses whereas the inner layer, harboring larger vessels, appears rather normal. 3-D reconstructions of 120 confocal sections demonstrate the almost complete lack of the outer plexiform vascular layer in VEGF-A$^{nescre/+}$ (J) compared with wild type retinas (I). Individual capillary loops in the intermediate layer and faint regressing profiles in the outer layer can be seen in the mutant retinas (arrowheads in H and J).

Fig. 1. Recombination specificity of the Nestin-Cre transgenic line. (A) Enhanced Green Fluorescent Protein (EGFP) visualized in an E12.5 Nestin-Cre;Z/EG double transgenic embryo, in which the two transgenes were inherited from different parents. The embryo shows brain and spinal cord-specific EGFP expression. (B) Ubiquitous EGFP expression in E12.5 Nestin-cre;Z/EG embryo in which both transgenes were transmitted from the same parent. (C) Schematic depiction of VEGF-A genomic locus. The black rectangular box marks the position of the *Xba*I (X)–*Bgl*II (B) genomic probe used in Southern analysis (D). The black "A" represents *Acc*I sites that are not polymorphic in the mouse. The red "A" represents a polymorphic *Acc*I site (RFLP) within Exon 3. (D) Southern analysis of DNA isolated from an 8-month-old VEGF-A$^{nescre/+}$ male. The wt allele lacks while the VEGF-A^{loxP} allele contains the *Acc*I site within exon 3, therefore generating a 4.8-kb and a 1.4-kb band, respectively. When the loxP-flanked exon 3 was removed from the conditional allele, the *Acc*I band size changed to 3.2 kb. a, cerebral cortex; b, cerebellum; c, heart; d, stomach; e, spleen; f, liver; g, intestine; h, sperm DNA from testis; i, kidney; j, bladder.

Murine VEGF-A is transcribed from a single gene that is alternatively spliced to produce at least three mRNA species, encoding for three proteins: VEGF-A120, VEGF-A164, and VEGF-A188 (Ng et al., 2001; Tischer et al., 1991). These VEGF-A isoforms are thought to establish VEGF-A gradients as a result of their individual binding capacity to the extracellular matrix. These gradients have been suggested to play a role in vessel patterning (Ruhrberg et al., 2002). In addition to alternate splicing, VEGF-A is controlled by hypoxia and exhibits a dynamic, temporal, and cell-specific pattern of expression (Dor et al., 2001; Miquerol et al., 1999).

At the early stages of vascularization of the developing brain, VEGF-A is expressed in the subventricular zone (Breier et al., 1992), while its receptors are expressed in endothelial cells of the perineural capillary plexus and capillary sprouts, infiltrating into the neuroectoderm (Dumont et al., 1995; Millauer et al., 1993). This expression pattern is suggestive of a role of VEGF-A and Flk1 in the directed growth of blood vessels into the developing brain. As the cortex develops, the neurons are the predominate source of VEGF-A (Ogunshola et al., 2000). VEGF-A expression is initially concentrated in the more superficial layers of the cortex and becomes more diffuse in the deeper layers as the animal reaches its third postnatal week (Ogunshola et al., 2000). When vascular remodeling is complete, VEGF-A expression switches to astroglia that stabilizes the mature vessels, while neuronal expression is reduced to basal levels (Ogunshola et al., 2000).

Astrocytic sources of VEGF-A are believed to play a pivotal role in the recruitment of the vasculature into the avascular retina of the newborn (Provis et al., 1997; Stalmans et al., 2002). The inner retinal vascular layer develops first, extends toward the periphery, remodels into arteries and veins, and through a process of sprouting angiogenesis penetrates the developing retina and forms the outer retinal vascular layer (Provis et al., 1997; Stalmans et al., 2002).

Several intriguing similarities and interrelationships have been documented between the developing nervous and vascular systems (Shima and Mailhos, 2000). They both form dense networks throughout the entire body. Active guidance systems are operational for both systems, and the initial primitive networks go through remodeling and maturation processes in tandem. The two systems share cofactors or receptors for signaling, such as the Ephrins (Adams and Klein, 2000; Kullander and Klein, 2002; Orioli and Klein, 1997) and Neuropilin-1. Neuropilin-1 has been demonstrated to play a pivotal role in neuronal guidance and also acts as a cofactor for VEGF-A164-mediated Flk1 signaling (Neufeld et al., 2002; Soker et al., 1998). Furthermore, in vitro experimentation has demonstrated a more direct role for VEGF-A/Flk1 in several aspects of neuronal biology. VEGF-A rescues neuronal cultures from ischemic and glutamate-induced neurotoxicity (Jin et al., 2000; Matsuzaki et al., 2001) and acts like a neurotrophic factor in stimulating axonal outgrowth (Sondell et al., 2000). These results suggest that VEGF-A may have a direct autocrine effect on neurons and glial cells. Exogenous addition of VEGF-A to the developing CNS results in improved intraneural angiogenesis, leading to increased neurogenesis and enhanced nerve regeneration after axotomy (Hobson et al., 2000; Jin et al., 2002). From a clinical perspective, altered VEGF-A levels and vascular development have been associated with neurodegenerative disorders, ischemic cerebral and spinal cord injury, and diabetic and ischemic neuropathy (Carmeliet and Storkebaum, 2002). In these situations, VEGF-A is thought to modulate neuronal development and function indirectly through its paracrine effects on the vasculature that in turn provides the necessary neurotrophic support for proper CNS development and homeostasis.

In this study, we have utilized the neural-specific conditional inactivation of both VEGF-A and its main receptor Flk1, to distinguish between autocrine versus paracrine modes of VEGF-A action in the nervous system. We have concentrated our analysis on retinal and cortical development in the mouse to address the potential functions of VEGF-A in these tissues. We have utilized the Nestin-Cre transgenic line in combination with a conditional and a hypomorphic VEGF-A allele to specifically lower VEGF-A levels in the developing CNS (Damert et al., 2002; Gerber et al., 1999; Tronche et al., 1999). To address the potential autocrine role of VEGF-A, Flk1 was conditionally inactivated by the Nestin-Cre transgene.

Through this genetic approach, together with a detailed high resolution analysis of the vascular endothelium, we have determined the phenotypic consequences of decreasing VEGF-A activity in cortex development and revealed specific alterations in the vascularization of the retina. This study suggests a dominant paracrine role for this factor in the structural organization of the nervous system.

Materials and methods

Mice

The Tie2-Cre, Nestin-Cre, Z/EG, conditional and hypomorphic VEGF-A mouse lines have all been previously reported (Kisanuki et al., 2001; Tronche et al., 1999; Novak et al., 2000; Gerber et al., 1999; Damert et al., 2002). Wild type ICR mice were obtained from Harlan, USA. All experiments were performed in accordance with protocols approved by our Animal Care Committee. Generation of the targeting vector and ES cell lines used to produce the conditional *Flk1* allele has been described previously (Muhlner et al., 1999). R1 ES cells harboring the conditional *Flk1* allele (see Supplementary Data) were injected into C57BL/6 blastocysts in order to generate chimaeric mice. One ES cell line (2C6) gave rise to chimaeric mice that transmitted the floxed *Flk1* allele through the germline, and this mouse line was maintained on a mixed C57BL/6-CD1 background.

Southern and PCR analysis

Genomic DNA isolated from adult male VEGF-A$^{nescre/+}$ organs and yolk sacs from E9.5 embryos were subjected to *Acc*I enzymatic digestion (NEB, Canada), separated by agarose gel electrophoresis transferred to a Hybond-N$^+$ membrane (Amersham-Pharmacia Biotech, Canada). The membrane was probed with an *Xba*I–*Bgl*II probe (corresponding to intron2 sequences upstream of Exon3) isolated from a plasmid containing an 18-kb genomic VEGF-A clone encompassing exons 1–4 of the murine VEGF-A locus (Ferrara et al., 1996). PCR analysis of the Nestin-Cre, Tie2-Cre, conditional and hypomorphic VEGF-A alleles have all been previously reported (Damert et al., 2002; Gerber et al., 1999; Kisanuki et al., 2001; Tronche et al., 1999). Genotyping of the conditional *Flk1* allele was performed on purified tail or embryonic yolk-sac DNA by using the primer pair UMCRE1 and UMCRE2 (oligonucleotide sequences 5′→3′-UMCRE1-GGGTGCCATAGCCAATCAAAGACGC; UMCRE2-TATCGGTGTTCCCCTGGGTGTGTGG) with the following PCR conditions: 1: 94°C for 90 s, 2: 94°C for 30 s; 3: 53°C for 40 s, 4: 65°C for 60 s; 39× to step 2. All PCR reactions were carried out by using PCR reagents from Bio Basics Inc. (Canada) according to manufacturer's instructions.

Histological analysis, TUNEL assay, BrdU and Hypoxia immunohistochemistry

Embryos from Nestin-Cre, VEGF-A$^{hypo/+}$ × VEGF-A$^{lox\text{-}P/lox\text{-}P}$ breedings were either dissected in ice-cold PBS, or brains and eyes were harvested at birth, P7, or P21 and fixed overnight at 4°C in 4% PFA. Samples for histological analysis were dehydrated through a graded alcohol series and embedded in paraffin wax as previously described (Haigh et al., 2000). Seven-micrometer sections were deparaffinized and either stained with Harris' Haematoxylin and Eosin or were subjected to either TUNEL assays, immunohistochemistry, or isolectin-B4 immunofluorescence analysis. TUNEL analysis was performed by using the in situ cell death detection kit (Roche, 1684809) according to the manufacturer's instructions. Prior to sacrificing the pregnant female mice, they were IP injected with a mixture of 50 mg BrdU (Sigma, B-9285) and 60 mg of pimonidazole hydrochloride (Hypoxyprobe hypoxia assay kit; NPI Inc., Belmont, MA) per kg mouse body weight (reagents were dissolved in 10 mM Tris/HCl, pH 7.4, 0.8% NaCl, 0.25 mM EDTA). Pregnant females were sacrificed 2 h following injections, and embryos were harvested and processed. Immunohistochemical analysis was performed as previously published by using an anti-BrdU antibody (Roche, Cat. No. 1170376) and an antibody raised against pimonidazole adducts (NPI, Inc.) (Behrens et al., 2003; Lee et al., 2001).

GFP, Isolectin-B4 analysis and confocal fluorescence microscopy

EGFP from the Nestin-Cre, Z/EG double transgenic embryos was detected as previously described (Novak et al., 2000). Embryos and eyes were fixed in 4% PFA in PBS at 4°C overnight and washed in PBS. Forebrains were dissected clean from surrounding tissue, labeled as described below, and flat-mounted ventricular side up. Retinas were dissected and cleared from retinal pigment epithelium, sclera, and hyaloid vasculature. Retina and forebrain samples were permeabilized in PBS containing 1% BSA and 0.5% Triton X-100 at 4°C overnight. They were rinsed in PBS, washed twice in PBlec (PBS, pH 6.8, containing 1% Triton X-100, 0.1 mM $CaCl_2$, 0.1 mM $MgCl_2$, 0.1 mM $MnCl_2$), and incubated in biotinylated isolectin B4 (*Bandeiraea simplicifolia*, Sigma L-2140), 20 μg/ml in PBlec at 4°C overnight. Following five washes in PBS, the samples were incubated with streptavidin conjugates (Cy3, Sigma) diluted 1:100 in PBS containing 0.5% BSA and 0.25% Triton X-100 at 4°C for 6 h. After washing and brief postfixation in 4% PFA, the retinas were directly flat mounted by using Mowiol supplemented with anti-bleaching agent DABCO (Sigma). Flat mounting of retinas was achieved by making four radial incisions. Retinas were analyzed by conventional fluorescence microscopy using a Nikon E1000 microscope equipped with a digital camera (Nikon Coolpix 990) and by confocal laser scanning microscopy using a Leica LCS NT. Digital images were processed by using Adobe Photoshop 6. Computer modeling of the retinal vasculature was performed with OpenLab software (version 2.0.7).

Vessel and neuronal quantification

Vessel quantification was performed by randomly counting branchpoints and calculating averages from five different randomly chosen fields from three separate mice per genotype at 160× magnification. Neuronal numbers and their proliferation indices were quantified by counting haematoxylin-stained neuronal nuclei and/or BrdU-labeled nuclei at 500× magnification in randomly chosen fields in the superficial cortical layers of the P21 brain and the periventricular zone of the developing cortex. Counts were performed on serial sections throughout representative mutant and control brains and embryos.

Results

Nervous system deletion specificity of the Nestin-Cre transgenic mouse line

Given the strong dosage sensitivity of the developing cardiovascular system to alterations in VEGF-A levels, one of the most critical initial issues was to confirm the exci-

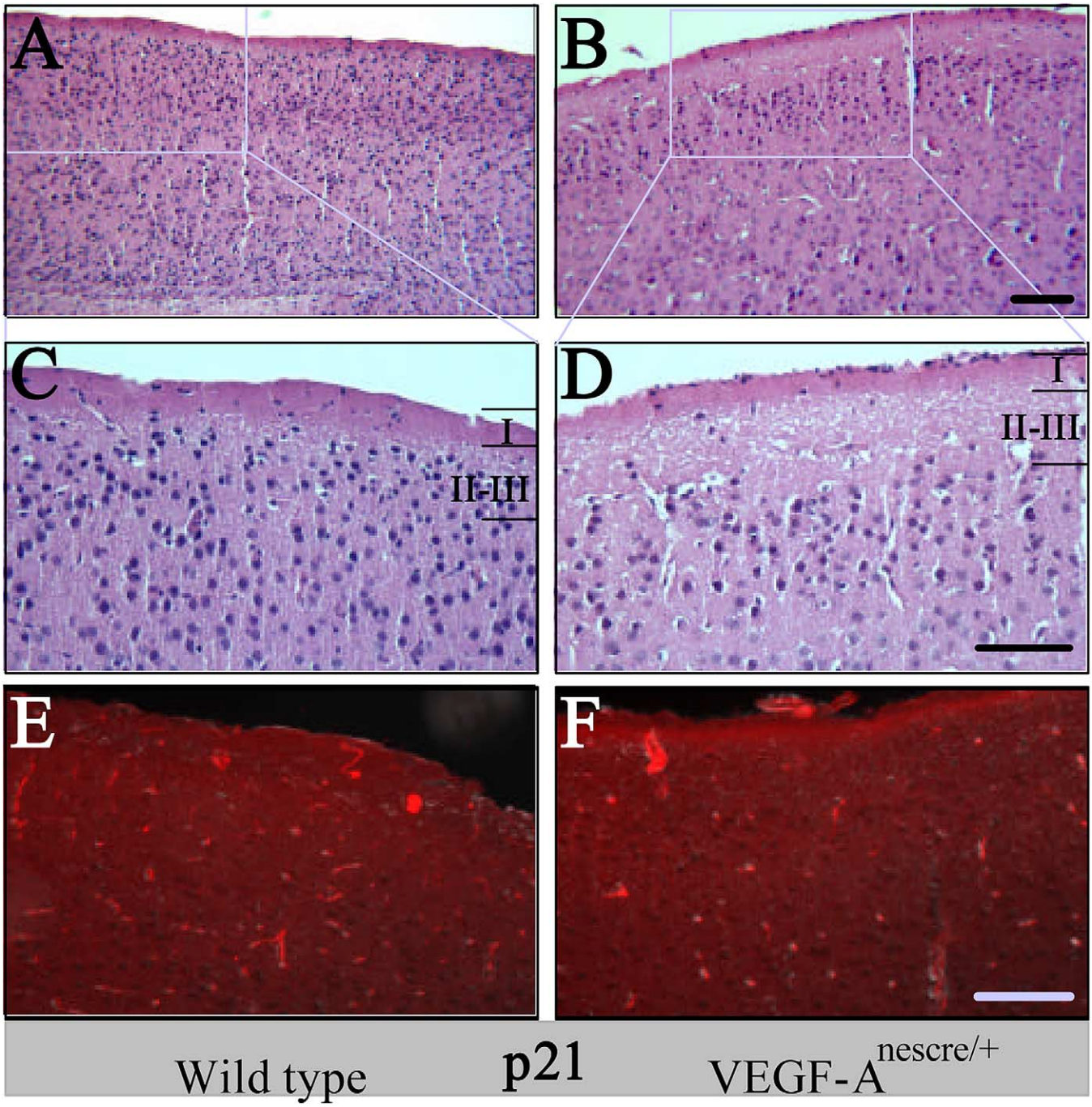

Fig. 3. Neuronal acellularity in the wild type and VEGF-A$^{nescre/+}$ cerebral cortex correlates with decreased sprouting angiogenesis. H&E histological staining through the cortical layers of wild type (A) and VEGF-A$^{nescre/+}$ (B) P21 mice. (C) and (D) are higher power images of the corresponding inserts showing the position and the cellularity of layers I–III. (E, F) Isolectin-B4 immunofluorescence staining on adjacent sections revealed decreased vascular density and decreased sprouting complexity in the P21 VEGF-A$^{nescre/+}$ cortex (F) compared with a littermate wild type control (E). Scale bars represent 50 μm.

sion-specificity of the Nestin-Cre transgene (Tronche et al., 1999). Therefore, Nestin-Cre transgenic mice were crossed with Z/EG reporter partners (Novak et al., 2000). In the double transgenic offspring, the Cre recombinase-mediated excision of the reporter transgene switched lacZ to Enhanced Green Fluorescent Protein (EGFP) expression, which gave a convenient readout of Cre expression specificity. E9.5 double transgenic embryos showed strong EGFP expression in the neuroectoderm, demonstrating the early onset of Cre activity in the CNS (data not shown). Three days later, E12.5 embryos showed strong EGFP expression exclusively along the entire length of the developing spinal cord and brain (Fig. 1A). To further characterize this line, Nestin-Cre; Z/EG double transgenic males or females were crossed with wild-type partners. Surprisingly, the resultant double transgenic embryos were ubiquitously green, indi-

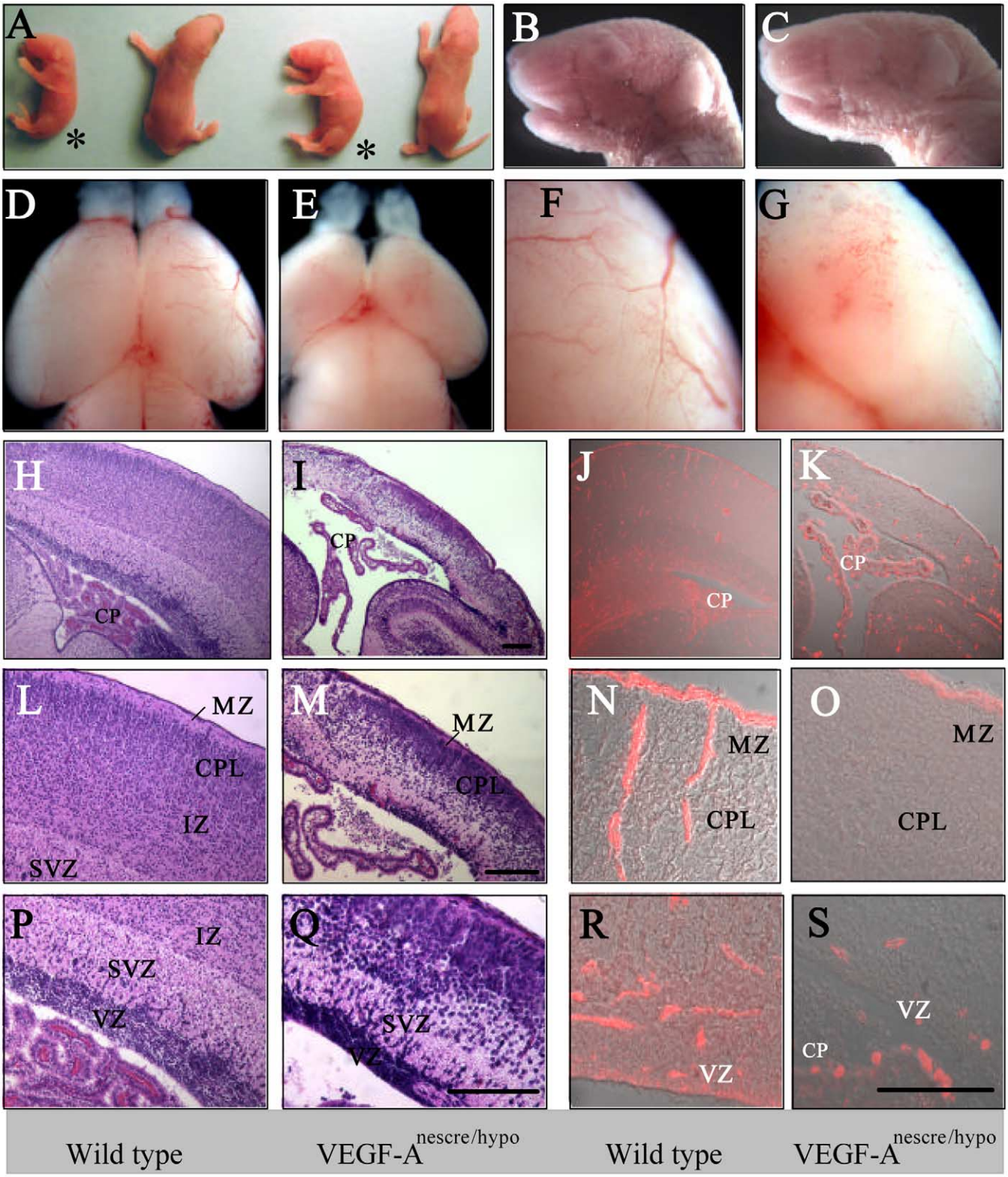

Fig. 4. Cortical neuronal degenerative phenotype of VEGF-A $^{nescre/hypo}$ neonates. (A) Posture of wild type and VEGF-A$^{nescre/hypo}$ neonates (asterisk). Cranial morphology of wild type (B) and VEGF-A$^{nescre/hypo}$ (C) newborns. The size of the wild type (D) and VEGF-A$^{nescre/hypo}$ (E) cerebral cortex and their corresponding pial vasculature (F and G, respectively). H&E staining of wild type (H, L, P) and VEGF-A$^{nescre/hypo}$ (I, M, Q) cortical sections. Note the expansion of the lateral ventricles (I). Isolectin-B4 endothelial immunofluorescence staining of wild type (J, N, R) and VEGF-A$^{nescre/hypo}$ cortex (K, O, S). Note the overall decrease in endothelial content and lack of sprouting angiogenesis from the pial vasculature in the mutant brain (O vs. N), CPL, cortical plate; MZ, marginal zones; VZ, ventricular zone; SVZ, subventricular zone; MZ, marginal zone; CPL, choroid plexus; IZ, intermediate zone. Scale bars represent 50 μm.

cating that ectopic Cre protein expression had mediated a premature excision of the reporter allele, presumably during gametogenesis (Fig. 1B). This unexpected "ectopic" germline excision of the reporter allele excluded the use of the Nestin-Cre transgenic mouse line for generating a complete nervous system-specific knockout of VEGF-A, while keeping the status of this gene wild type in other tissues. This is necessary, since the ubiquitous deletion of one of the conditional VEGF-A alleles leads to early embryonic lethality (Carmeliet et al., 1996; Ferrara et al., 1996).

To generate mice that have deleted one VEGF-A allele specifically in the developing nervous system, Nestin-Cre hemizygous transgenic mice were crossed with partners homozygous for the VEGF-A conditional allele (VEGF-$A^{loxP/loxP}$) (Gerber et al., 1999). Double transgenic Nestin-Cre; $VEGF^{loxP/+}$ mice (hereafter referred to as VEGF-$A^{nescre/+}$ mice) were born with the expected Mendelian frequency and showed no overt phenotypical or behavioral abnormalities under normal conditions (data not shown). To determine the specificity and efficiency of Nestin-Cre-mediated deletion of the floxed VEGF-A allele in the double transgenic mice, Southern analysis was performed on tissues isolated from an 8-month-old adult male mouse. This analysis depicted the high degree of deletion of the conditional VEGF-A allele in the cerebrum and cerebellum (a and b, respectively, in Fig. 1D). All other tissues examined with the exception of sperm isolated from the testis of this mouse showed no or only minimal excision of this allele (Fig. 1D). The complete excision of the conditional VEGF-A allele in sperm was consistent with our characterization of Nestin-Cre expression using the Z/EG reporter and further supported our initial observations that the Cre protein is also expressed during gametogenesis.

Delays in vascular remodeling and outer retinal vascular layer deficiencies in VEGF-$A^{nescre/+}$ mice

At postnatal day 1 (p1), we did not observe any differences in vessel invasion into the inner retinal layer from the optic disc in the VEGF-$A^{nescre/+}$ mice compared with wild type controls (data not shown). By p7, the wild-type vasculature has almost reached the periphery and has commenced vascular remodeling and specification resulting in an alternating pattern of properly interconnected branching arteries and veins (a and v in Fig. 2A). The retinas from VEGF-$A^{nescre/+}$ mice show normal vascular migration and extension into the periphery compared with controls. However, substantial delays in vascular remodeling are indicated by the abnormally high vascular plexus density ahead of the developing arteries (asterisk in Fig. 2B). Occasionally, arteries and veins cross-over (arrows in Fig. 2B and F). 3-D computer generated shadow projections of isolectin-B4-labeled endothelium show filopodial extension toward the periphery in both wild type and VEGF-$A^{nescre/+}$ retinas at p7 with slight increases in aberrantly orientated filopodia in the heterozygous VEGF-A mutant (arrowheads in Fig. 2C and D). Between p5 and 3 weeks of age, the retinal vasculature invades the retina and forms a complex tripartate vascular plexus "sandwiching" parts of the retina between an inner and outer vascular layer (Fig. 2G). In the most affected mutant retinas, there was a clear lack of development of the outer retinal layer in VEGF-$A^{nescre/+}$ mice by p21 of development (Fig. 2E–J). At p21, the control retina displays a normal alternating pattern of arteries (a) and veins (v), and the veins are never directly connected to capillaries of the inner retinal plexus but receives input from the outer capillary plexus (Fig. 2E, G, and I). Mutant p21 VEGF-$A^{nescre/+}$ retinas that lacked a proper outer vascular plexus (Fig. 2F, H, and J) were extremely thin and showed signs of degeneration (data not shown). Not all retinas were as severely affected: retinal thickness correlated with the degree of formation of the outer capillary plexus. In keeping with the retinal degenerative phenotype, we also observed a strong increase in microglia/macrophage numbers near the developing veins in some mutant retinas already at p7 (Supplementary Data, Figure I). This increased microglial density is consistent with gliosis and retinal degeneration. The lack of an outer vascular plexus in affected mice is also reflected in the numerous connections of the inner capillary plexus to veins, and frequently, arteries and veins continue to crossover (white arrow in Fig. 2F). 3-D computer generated reconstructions of the isolectin-B4 immunofluorescence images of the retinal vasculature show that in the control retina there are normal larger vessels in the outer plexiforme layer below the inner retinal layer (Fig. 2G). In the most affected mutant p21 retinal vasculature, 3-D overviews show a normal inner vascular layer but a clear lack of development of the outer plexiforme layer (Fig. 2H). Computer-assisted side views (Z-views) of reconstructions of 120 serial confocal images unequivocally demonstrate the differences in retinal vasculature between wild type and the mutant (Fig. 2I and J).

Altered vascular development leads to cortical acellularity in VEGF-$A^{nescre/+}$ mice

Gross inspection of wild type and VEGF-$A^{nescre/+}$ brains revealed no overall changes in patterning. We observed, however, a substantial reduction (approximately 20–30%) in overall cortical brain size in VEGF-$A^{nescre/+}$ brains compared with age- and sex-matched wild type littermates by p21 (data not shown). Histological inspection of the mutant cortex revealed an overall decrease in neuronal cellularity, particularly in the more superficial cortical layers I–III (Fig. 3A–D). To quantitate this decrease, we counted randomly selected fields in these regions at 500× magnification every fifth section (~35 μm) from five different serial sections throughout representative mutant and control brains. Neuronal counts at p21 revealed a mean of 53 ± 18 neurons in the control cortical layer I and 19 ± 8 neurons in the VEGF-$A^{nescre/+}$ cortex. Cortical layers II and III showed even greater differences in neuronal cellularity with wild

type neuronal counts being on average 104 ± 35 and mutants counts being 35 ± 10 cortical neurons per optical field. Isolectin-B4 immunofluorescence analysis of brain sections revealed an overall decrease in vascular density and sprouting angiogenesis that was not only limited to the cortex but also present in the cerebellum, brain stem, and spinal cord (data not shown).

Severe reductions in VEGF-A activity causes neuronal degeneration of the cortex

To further decrease VEGF-A levels below those obtained in VEGF-A$^{nescre/+}$ mice in the developing nervous system, a hypomorphic VEGF-A allele (VEGF-A^{hypo}) (Damert et al., 2002) was bred into this genetic system. Since mice heterozygous for the hypomorphic allele are viable, Nestin-Cre; VEGF-A$^{hypo/+}$ double transgenic males were first generated and then mated with VEGF-A$^{loxP/loxP}$ partners to produce Nestin-Cre; VEGF-A$^{loxP/hypo}$ triple transgenic offspring. In these mice, one of the VEGF-A alleles is specifically deleted in the developing nervous system, while the other is hypomorphic throughout the mouse. Therefore, outside the nervous system, the VEGF-A status of these animals is functionally equivalent with that of the VEGF-A$^{+/hypo}$ viable genotype. Hereafter, these offspring are designated as VEGF-A$^{nescre/hypo}$ mice.

VEGF-A$^{nescre/hypo}$ mice were born alive in the expected Mendelian ratio, but they could not survive beyond p1. These neonates were readily identifiable phenotypically from their wild type littermates by their altered cranial morphology and spastic uncontrolled movements (Fig. 4A–C, and data not shown). They displayed an inability to remain upright when placed in the prone position likely as a result of a lack of muscular coordination (Fig. 4A) and were unable to feed as was evidenced from the absence of milk in their stomachs. They died of dehydration within 24 h (Fig. 4A, and data not shown). Dissections of wild type and mutant p1 brains show a clear difference in the size of cerebral cortex in the mutant VEGF-A$^{nescre/hypo}$ mice (Fig. 4D and E). Higher power magnification of mutant cortices showed an absence of pial vasculature and evidence of cortical degeneration compared to control littermate cortices (Fig. 4F and G). Closer histological inspection of the mutant brain revealed altered cortical neuronal organization and accompanying neuronal degeneration mainly in the subventricular zone (SVZ in Fig. 4Q). In contrast, the wild type brain showed typical well-organized cortical zones (Fig. 4H, L, and P). In addition to the anterior cortical degenerative phenotype, there was also evidence of hydrocephalus (excess cerebrospinal fluid) and altered choroid plexus (cp) development and function (Fig. 4I). Isolectin-B4 immunofluorescence analysis of the cortical brain vasculature demonstrated a severe deficiency in vascular development in both the superficial levels of the cortex near the marginal zone (mz) and cortical plate (cpl), and in the deep ventricular zone (vz) in the mutant VEGF-A$^{nescre/hypo}$ brain compared with controls (Fig. 4K, O, and S, compared with wild type seen in Fig. 4J, N, and R). Vessel analysis of other regions of the CNS showed similar defects in vessel density; however, no obvious neurodegenerative phenotypes were evidenced as in the cerebral cortex (data not shown).

Altered VEGF-A levels cause dosage-dependent reductions in vessel density

In order to gain insights into how altered VEGF-A levels affect vessel patterning in the p1 cortex, we examined thick vibratome sections using immunofluorescence analysis of the isolectin-B4-labeled vasculature. Average vessel branching point density was determined for the wild type, VEGF-A$^{nescre/+}$, VEGF-A$^{hypo/+}$, and VEGF-A$^{nescre/hypo}$ genotypes as 5430 (100%), 3386 (40%), 3196 (37%), and 477 (9%) branch points/mm^2 (Fig. 5A–D). The reductions in branch points resulted in greater distances between blood vessels. In the wild type, there is an average distance of 50 μm between vessels that rises to 70 μm in the VEGF-A$^{nescre/+}$ and VEGF-A$^{hypo/+}$ samples and is up to 100 μm in the most severe VEGF-A$^{nescre/hypo}$ cortex in vascularized areas. The mutants also showed changes in sprouting endothelial tip-cell morphology in terms of filopodial extensions. In the wild type, long filopodia extend in a directional manner only from the leading endothelial tip-cell (insert in Fig. 5A). In the VEGF-A$^{nescre/+}$ cortices, the sprouting tip cell morphology was quite normal; however, small ectopic non-tip-cell filopodia could be observed in large vessels (insert, Fig. 5B; and data not shown). In the VEGF-A$^{hypo/+}$ cortex, there were fewer tip-cell filopodia extensions that appeared longer and less spread out than in the wild-type controls, but showed little evidence of ectopic extensions (insert, Fig. 5C). In the VEGF-A$^{nescre/hypo}$ mutants, very little tip-cell filopodial sprouting could be observed at all, and when present on tip-cells, they appeared long and spatially confined as in the hypomorphic situation. The vessels that did exist in the double mutant appeared irregular with some small ectopic sprouting from the larger vessels (insert in Fig. 5D, and data not shown). In terms of the eye vasculature, there was also a clear absence of sprouting angiogenesis into the p1 inner plexiforme layer of the retina in the VEGF-A$^{nescre/hypo}$ mutants compared with the wild-type littermates. However, given the lethality of the double mutants at this time point, no further analysis could be performed (data not shown).

Given the early onset of Cre activity in the Nestin-Cre transgenic line (<E9.5), vascular density was also examined in both the affected forebrain region and the nondegenerated hindbrain region at E10.5 in all four genotypes (Fig. 5 and Supplementary Data, Figure II). In the wild-type forebrain vasculature as seen from the ventricular side, normal branching and vessel spacing is observed with long filopodial extensions arising solely from the sprouting tip-cell (Fig. 5E and F). The average number of branch points for the wild-type, VEGF-A$^{nescre/+}$, and VEGF-A$^{hypo/+}$ fore-

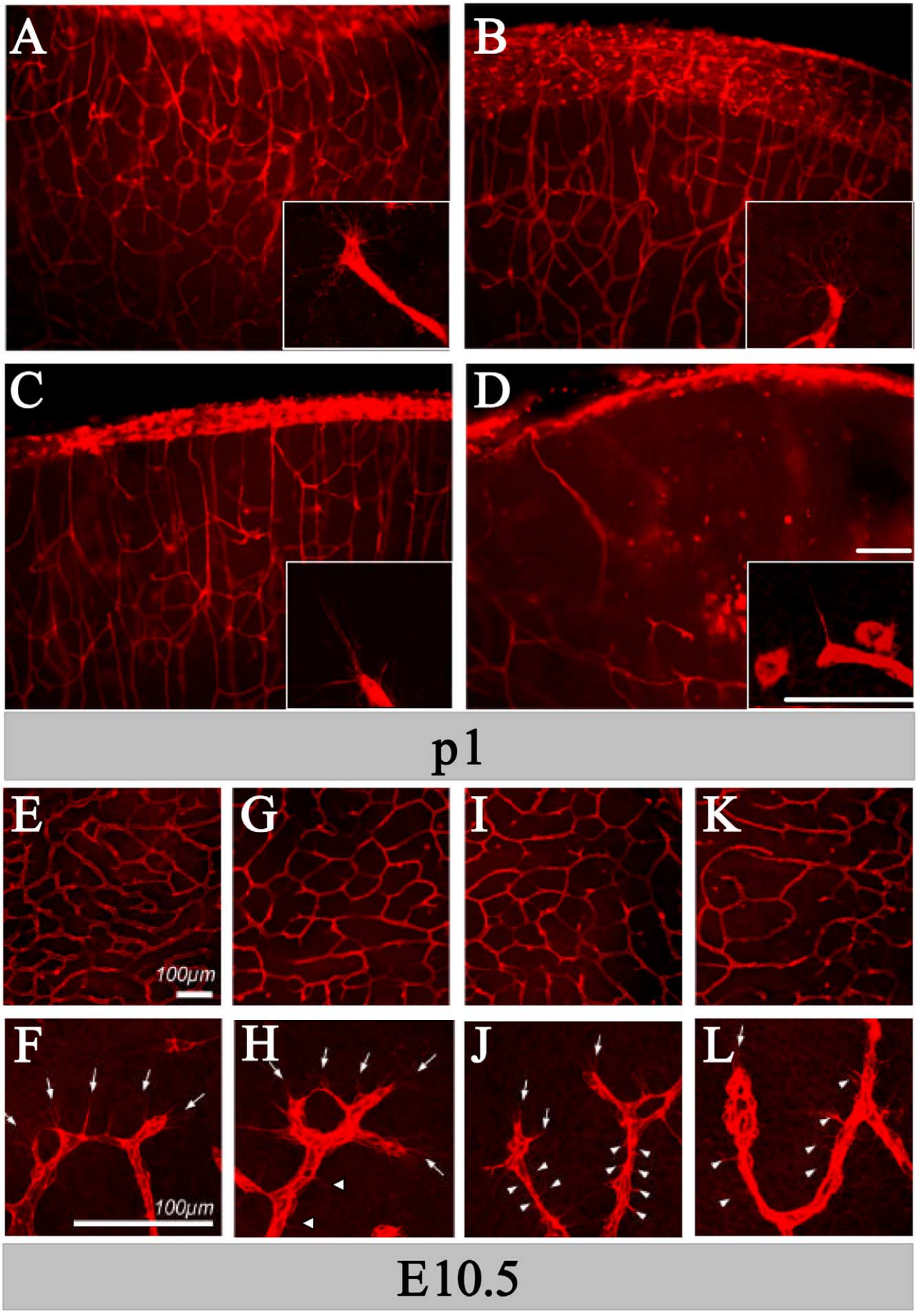
A
B
C
D
p1
E
G
I
K
100μm
F
H
J
L
100μm
E10.5

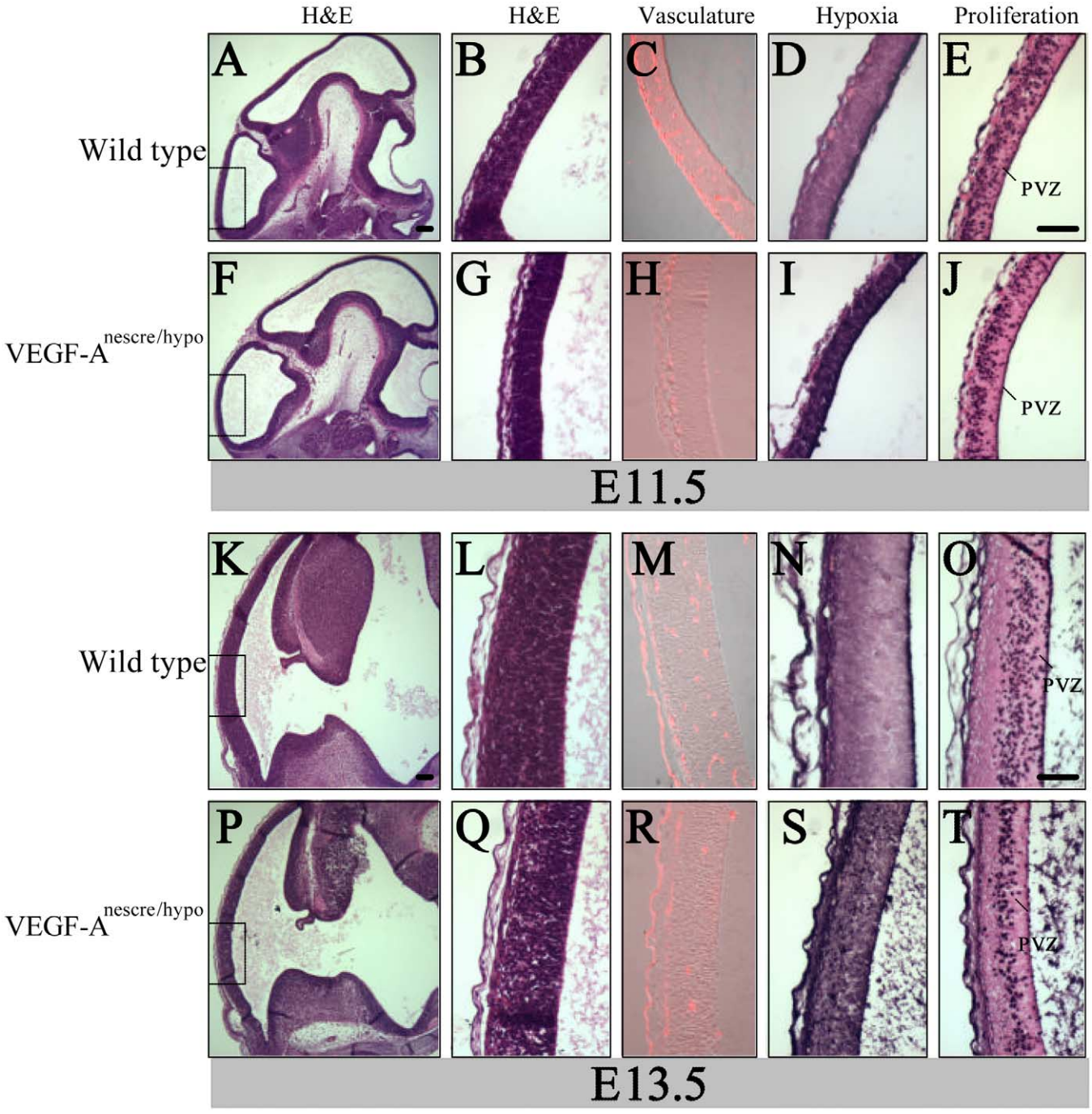

Fig. 6. Histological analysis of the forebrain of wild type (1st and 3rd rows, A–E and K–N) and VEGF-A$^{nescre/hypo}$ (2nd and 4th rows, F–J and O–S) E11.5 and 13.5 embryos for morphology (H&E staining, 1st column), cellularity (H&E staining, 2nd column), vascularization (Isolectin-B4 immunofluorescence, 3rd column), hypoxia (anti-pimonidazole immunohistochemistry, 4th column), and proliferation (BrdU labeling, 5th column). PVZ, periventricular zone. Scale bars represent 50 μm.

Fig. 5. Isolectin-B4 endothelial cell immunofluorescence staining of the p1 cortex and E10.5 flat-mount forebrains from four genotypes producing different levels of VEGF-A. In the order of increasing vascular defect severity: (A) wild type, (B) VEGF-A$^{nescre/+}$, (C) VEGF-A$^{hypo/+}$, and (D) VEGF-A$^{nescre/hypo}$ (160× magnification). Inserts are 630× magnifications of leading edge sprouting-tip endothelial cells. Note that in the wild type cortex, long filopodia extend from the tip cell (insert in A) and in VEGF-A$^{nescre/+}$ (insert in B) tip cell morphology is similar to the wild type. In VEGF-A$^{hypo/+}$ samples (insert in C), the filopodia number is slightly decreased and is most severe in the VEGF-A$^{nescre/hypo}$ cortex where very few filopodia were observed (insert in D). Vascular plexus (E) and sprouting endothelial cells (F) of wild type E10.5 forebrain. Note the normal endothelial branching and patterning and long bundles of filopodia extending from distinct regions of the developing tips, while the vessel surface remains relatively smooth and lacks non-tip cell filopodial extensions (white arrows). Vascular plexus (G) and sprouting endothelial cells (H) of VEGF-A$^{nescre/+}$ and VEGF-A$^{hypo/+}$ (I, J) forebrain. Note that these genotypes show intermediate levels of vessel branching densities and patterning defects compared with wild type. They also show filopodial extensions from ectopic non-tip cells (white arrowheads in H and J). In the VEGF-A$^{hypo/+}$ forebrain (J), the ectopic and tip-cell filopodia extensions are shorter than wild type and VEGF-A$^{nescre/+}$ filopodia. In VEGF-A$^{nescre/hypo}$ forebrains (K), the degree of vascular branching becomes markedly decreased. The length of filopodia extensions is decreased and ectopic extensions are prevalent and have a much more irregular surface and tuft-like morphology (L). Scale bars represent 100 μm.

brains was 221 (100%), 183 (83%), and 164 (74%) branch points/mm^2, respectively. As a result of this altered branching, the distance between vessels was also increased in a similar way as in the p1 cortex (Fig. 5G and I). In both heterozygous mutant samples, ectopic filopodial extensions are observed branching off on non-tip endothelial cells (arrowheads in Fig. 5H and J). In the VEGF-A$^{nescre/hypo}$ mutants, branching density fell further still to 87 (39%) branchpoints/mm^2 and displayed the accompanying increased distance between vessels (Fig. 5K). The vasculature in the double mutant showed non-tip cell filopodial extensions and in general the vasculature seemed much more irregular than either heterozygous mutant or wild type littermates (Fig. 5L). Overall, despite the differences in vessel branching and filopodial extensions, at this stage the vessel diameter remained the same in all four genotypes examined.

Altered vessel density causes abnormal neuroectoderm development

Histological, isolection-B4 vessel, hypoxia, apoptosis, and proliferation analyses were performed on adjacent sections of VEGF-A$^{nescre/hypo}$ mutant and wild-type embryos at E11.5, E13.5, and E15.5 time points to determine the onset of neuronal degeneration and the cellular mechanisms behind this phenotype (Figs. 6 and 7). At E11.5, no overt histological difference was observable between control and mutant (Fig. 6A, B and F, G, respectively). This is despite the clear differences seen in sprouting angiogenesis already present within this region (Fig. 6C and H). The hypoxia marker pimonidazole hydrochloride (Lee et al., 2001; Varia et al., 1998) was used to determine any differences in tissue hypoxia between control and mutant sections that correlated with the altered vessel phenotype. Clear differences were observed in the level of tissue hypoxia between controls and mutant samples, while no differences in neuronal apoptosis were observed by TUNEL analysis in the same tissues (Fig. 6D and I, and data not shown). The decreased vessel density and increased tissue hypoxia did have effects on neuronal proliferation in the periventricular zone (PVZ) of VEGF-A$^{nescre/hypo}$ mutant forebrains compared with controls (Fig. 6E and J). BrdU labeling demonstrated a 25% reduction in the numbers of proliferating neurons in the mutant periventricular zone (data not shown). The first clear histological evidence of degeneration became apparent in the mutant forebrain at E13.5 (Fig. 6P). Altered vessel densities and continued hypoxia resulted in a 60% decrease in the number of proliferating periventricular neurons in the mutant forebrains but still demonstrated no differences in neuronal apoptosis compared with controls (Fig. 6N and S, and data not shown). At E15.5, overt and specific anterior cortical neuronal degeneration was observed in histological sections of the VEGF-A$^{nescre/hypo}$ mutant brains (Fig. 7A and B). The decreased vessel density and lack of sprouting angiogenesis became more pronounced by E15.5, and there was ubiquitous hypoxia seen throughout the CNS in the mutant compared with controls (Fig. 7C, D and E, F, and data not shown). At this stage, TUNEL analysis revealed a large number of apoptotic neurons in the mutant cortex compared to controls (Fig. H vs G). The neuronal degeneration therefore starts between E13.5 and E15.5 and becomes more pronounced as development proceeds, with the first visible external differences in cranial morphology observable by E17.5 (data not shown).

Conditional inactivation of Flk1 in the developing nervous system does not result in overt changes in neuronal development

The specific aberrations in the development of cortical layers in the VEGF-A$^{nescre/+}$ mice and the severe neuronal degenerative phenotype observed in the VEGF-A$^{nescre/hypo}$ mutants raised the possibility that the putative autocrine role of VEGF-A in neuronal development may also have contributed to these phenotypes. To examine this possibility, we performed a nervous system-specific inactivation of the main signaling VEGF-A receptor, Flk1, using the Nestin-Cre transgenic line and a conditional *Flk1* allele (fully characterized in vitro; Muhlner et al., 1999, unpublished in vivo, see Supplementary Data, Figure III). Nestin-Cre, Flk1$^{loxP/+}$ double transgenic males were crossed with Flk1$^{loxP/loxP}$ homozygous females to produce Flk1$^{nescre/loxP}$ offspring. Given the excision specificity of the Nestin-Cre transgene described previously, these mice are deficient for Flk1 in the nervous system but heterozygous null in other cell types. In contrast to the VEGF-A$^{nescre/hypo}$ embryos, Flk1$^{nescre/null}$ embryos dissected at E13.5 showed no histological, apoptotic or proliferative abnormalities throughout the developing CNS (Fig. 8A–F, and data not shown). Flk1$^{nescre/null}$ mice were born in the normal ratio and showed no obvious behavioral phenotypes by 1 month of age (data not shown). Therefore, our analysis has failed to substantiate the putative autocrine role of VEGF-A/Flk1 signaling in nervous system development in vivo.

Discussion

In this study, we have addressed the specific role of VEGF-A in the developing nervous system through the combined use of a conditional gene inactivation approach and a hypomorphic VEGF-A allele. Through this strategy, we have been able to investigate how both intermediate and more severe reductions in VEGF-A levels affect vessel density in the developing cortex and retina.

The role of VEGF-A in vessel patterning has already been suggested in studies of VEGF-A isoform knockouts (Ruhrberg et al., 2002; Stalmans et al., 2002), where alternatively spliced exons were either removed or fused with cDNA fragments to enforce the production of only one of the three isoforms. In these approaches, changes in VEGF-A gradients and/or isoform-specific signaling are

suggested to cause the observed alterations in vascular patterning. However, in these studies, the effect of VEGF-A levels is rather difficult to identify since the removal of two of the three isoforms creates a situation where the remaining isoform is disproportionately overexpressed.

Our study demonstrates that both the nervous system-specific intermediate reduction (VEGF-$A^{nescre/+}$) or intermediate global reduction (VEGF-$A^{hypo/+}$) of VEGF-A resulted in alterations in vessel density but not diameter. The branching density in VEGF-$A^{nescre/+}$ and VEGF-$A^{hypo/+}$ newborns showed approximately 40% reductions, while the VEGF-$A^{nescre/hypo}$ neonates showed a 90% decrease in the cortex compared with controls. In contrast to what was observed in the VEGF-$A^{120/120}$ embryos (Ruhrberg et al., 2002), we did not find any differences in vessel diameter in any of the mutant genotypes examined. This difference could be attributable to the fact that there is a proportional overexpression of the VEGF-A120 isoform throughout the VEGF-$A^{120/120}$ embryos compared with the wild-type VEGF-A120 expression levels. However, at present there is no evidence for isoform-specific VEGF-A signaling being responsible for distinct responses in the vascular endothelium. A more favorable idea is that the lack of heparin binding VEGF-A isoforms changes the extracellular distribution of VEGF-A and thereby affects the balance between migration and proliferation, resulting in increased vessel diameter (Carmeliet et al., 1999; Ruhrberg et al., 2002). Simplistically, decreased migration and branching but normal or increased proliferation would lead to increased vessel diameter, whereas coordinated reduction of migration and proliferation would merely reduce vessel density. This idea is in agreement with the effect of reduced levels of VEGF-A (this study) and with the results of changed isoform distribution (Ruhrberg et al., 2002; Stalmans et al., 2002).

Accordingly, VEGF-$A^{120/120}$ mice demonstrated reduced migration of the vasculature into the developing inner retinal layer (2/3 of normal migration distance by P9) (Stalmans et al., 2002). Similarly, in the hindbrain, migration and branching were reduced, whereas proliferation was normal (Ruhrberg et al., 2002). In contrast, VEGF-$A^{188/188}$ mice (expressing only VEGF-A188), showed normal vessel outgrowth but increased capillary network density (Stalmans et al., 2002; Ruhrberg et al., 2002). Interestingly, Ruhrberg et al. (2002) found that the VEGF-$A^{164/164}$ and the *trans*-heterozygous VEGF-$A^{120/188}$ embryos developed normal vessel networks. They concluded that isoform specific signaling is unlikely to be an absolute requirement to specify proper branching patterns (Ruhrberg et al., 2002). Here, we show that intermediate and severe reductions in nervous system VEGF-A activity results in dosage-dependent changes in vascular density, but not vessel size or rate of endothelial migration.

Effect of altered vessel density on cortical and retinal development

Despite altered vessel density and increased hypoxia throughout the entire developing nervous system, we found a specific and severe degeneration of the cerebral cortex in VEGF-$A^{nescre/hypo}$ neonatal mice. VEGF-$A^{nescre/+}$ mice that have milder reductions in VEGF-A levels show signs of neuronal acellularity in the cortex and display a retinal degeneration phenotype that resembles certain forms of human retinopathies (Ferrara, 2002; Lu and Adamis, 2002; Smith, 2002). The cortical neuronal degenerative phenotype in VEGF-$A^{nescre/hypo}$ mice was 100% penetrant, while the phenotypes in the VEGF-$A^{nescre/+}$ mice varied. The molecular mechanisms responsible for this variability in the VEGF-$A^{nescre/+}$ mice, and for the specific increase in cortical neuronal apoptosis in the VEGF-$A^{nescre/hypo}$ neonates, remains to be determined. Hypoxia is likely to be an important factor, since it is a known modulator of neuronal apoptosis, and we have documented increased hypoxia throughout the developing nervous system from E11.5 onwards. VEGF-A is one of the best known and characterized hypoxia regulated genes (Semenza, 2001), showing rapid and strong upregulation in its expression in both cell culture settings and in vivo (Semenza, 2001). Compensatory upregulation of the wild-type VEGF-A allele due to tissue hypoxia may have resulted in the variability seen in the retinal vasculature and cortical phenotypes that we observed in this study. This could also explain the regional differences observed for ectopic filopodia extensions. Furthermore, differences in Cre-mediated VEGF-A excision and strain variance in this outbred system may also contribute to the observed variability.

Regional differences in the balance of the expression of pro- and anti-apoptotic genes in the brain can make neurons differentially vulnerable to hypoxic insults (Banasiak et al., 2000). This could be a possible explanation for the specific cortical neuronal apoptosis phenotype observed in developing VEGF-$A^{nescre/hypo}$ mice. As well, the lack of sprouting angiogenesis into the VEGF-$A^{nescre/hypo}$ cortex may have resulted in changes in the expression of specific neurotrophic factors (NF) released from the endothelium or other cell types in the cortex. This decrease in neurotrophic support would then be responsible for the decreased neuronal proliferation, aberrant neuronal migration, and increased neuronal apoptosis that we observed in the ventricular and subventricular regions of the developing cortex. This hy-

Fig. 7. Histological analysis of the forebrain of wild type (1st column: A, C, E, G) and VEGF-$A^{nescre/hypo}$ (2nd column: B, D, F, H) E15.5 embryos for cellularity (H&E staining, 1st row, A-B), vascularization (Isolectin-B4 immunofluorescence, 2nd row, C-D), hypoxia (anti-pimonidazole immunohistochemistry, 3rd row, E-F), and apoptosis (TUNEL assay, 4th row, G-H). Scale bars represent 50 μm.

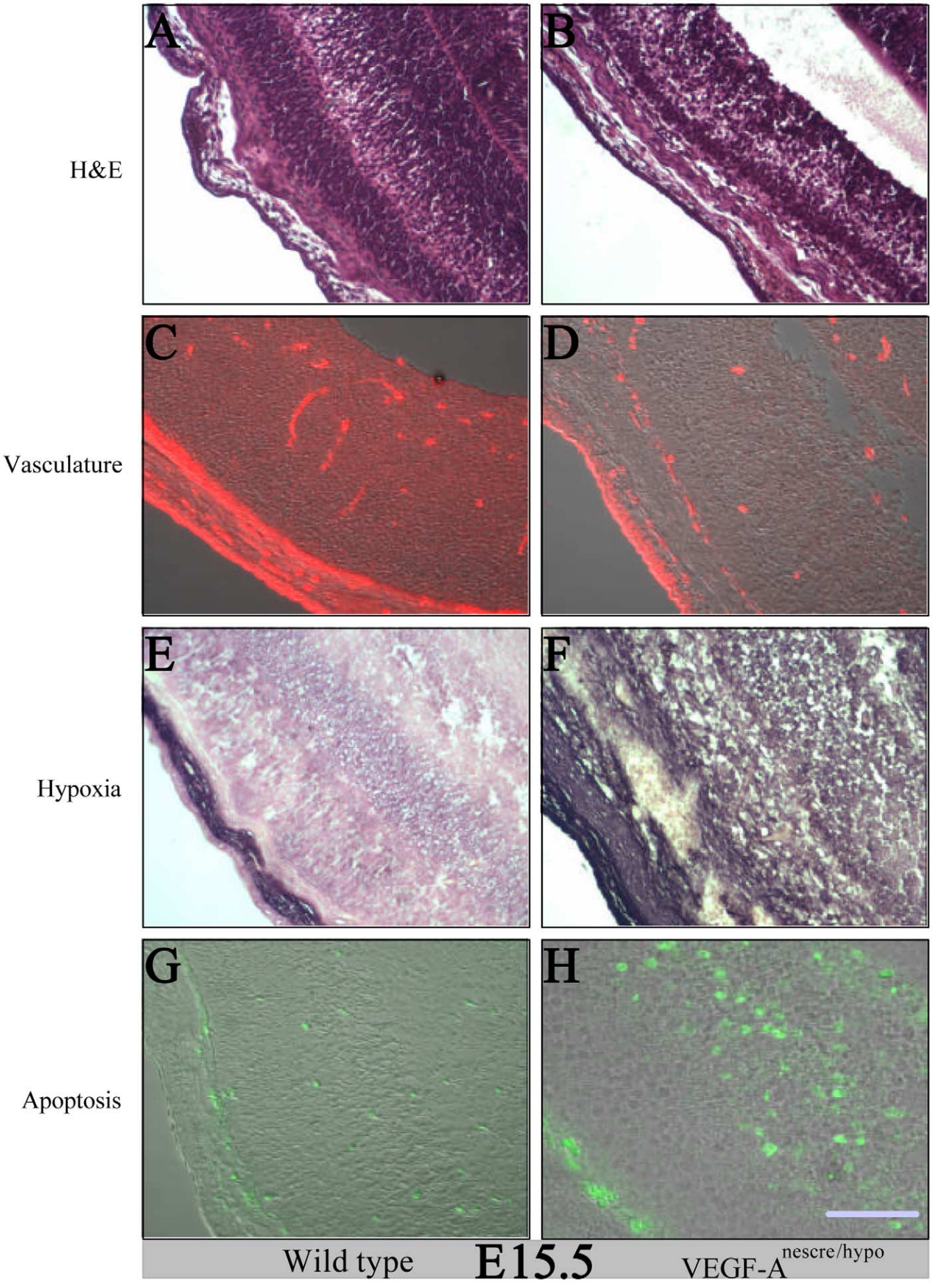
A
B
H&E
C
D
Vasculature
E
F
Hypoxia
G
H
Apoptosis
Wild type
E15.5
VEGF-A nescre/hypo

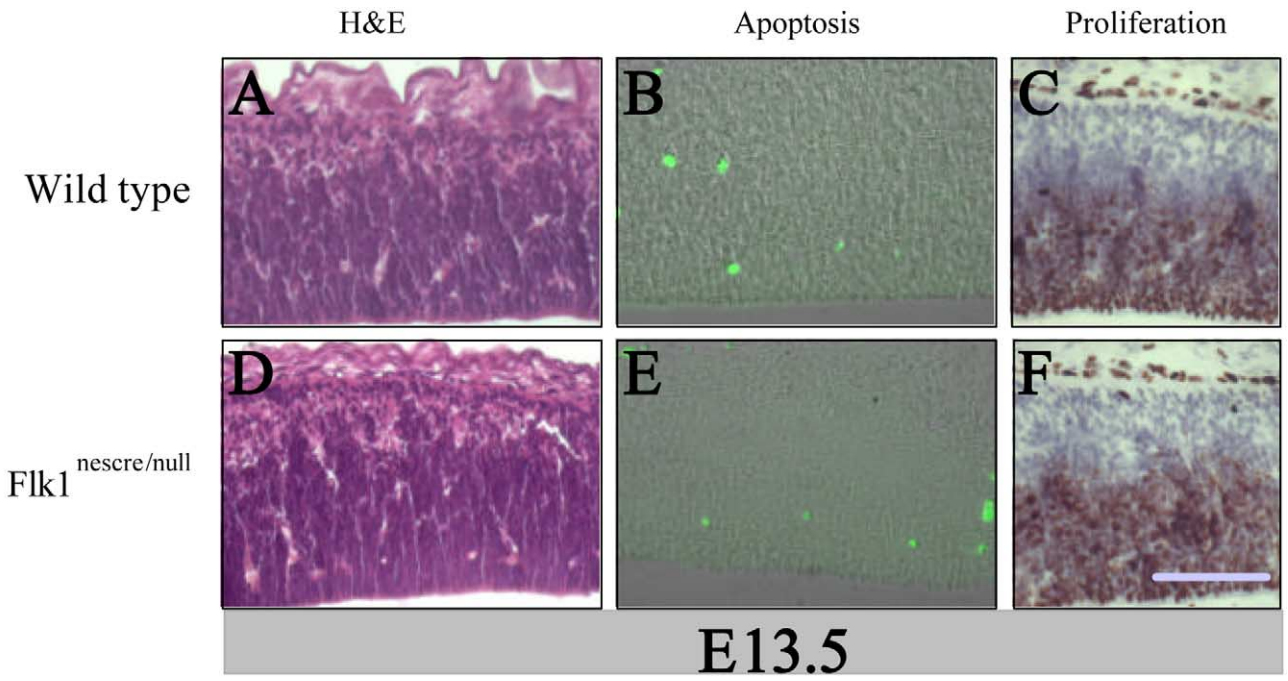
H&E
Apoptosis
Proliferation
A
B
C
Wild type
D
E
F
Flk1 nescre/null
E13.5

8

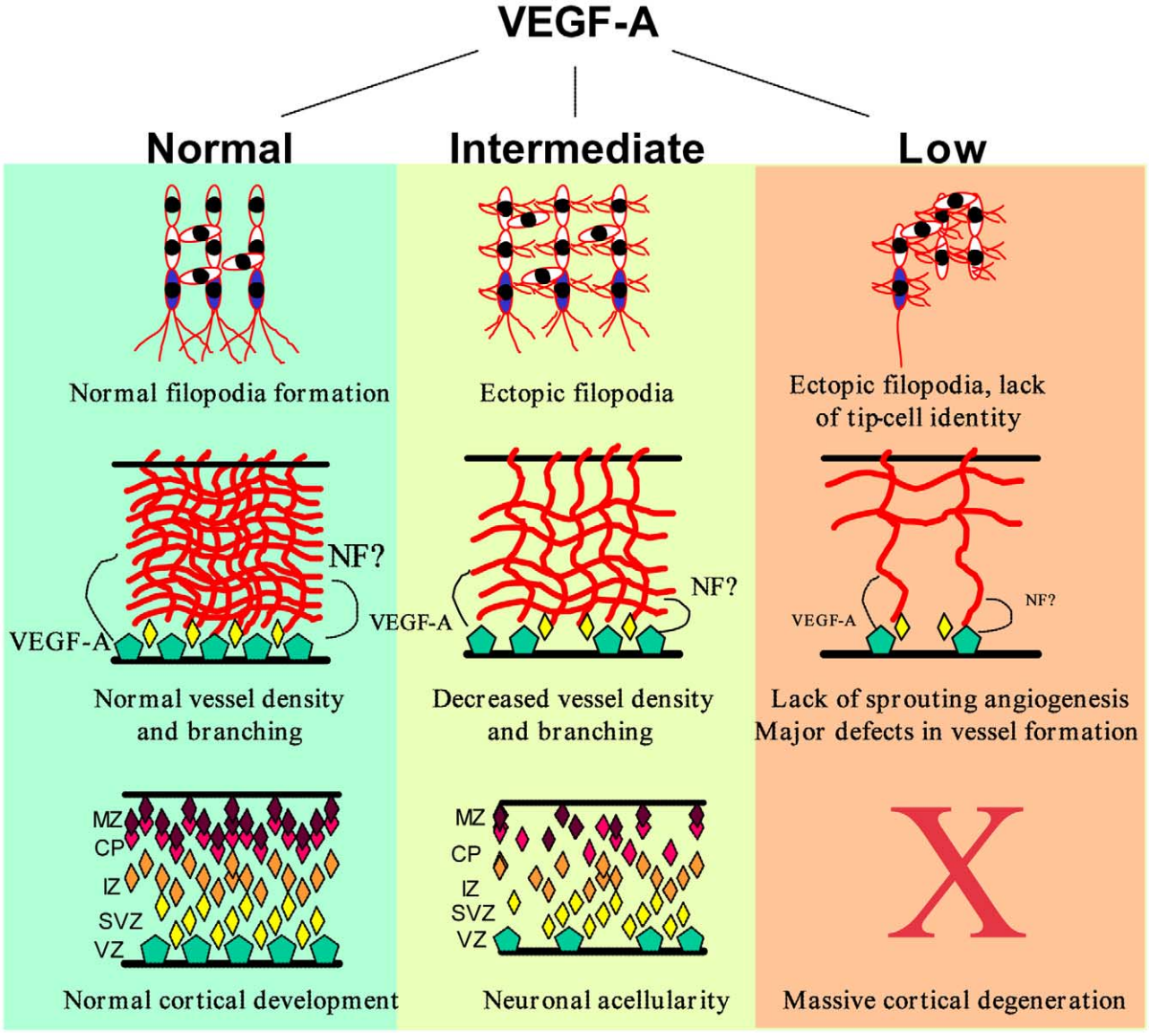
VEGF-A
Normal
Intermediate
Low
Normal filopodia formation
Ectopic filopodia
Ectopic filopodia, lack of tip-cell identity
NF?
VEGF-A
NF?
VEGF-A
NF?
VEGF-A
Normal vessel density and branching
Decreased vessel density and branching
Lack of sprouting angiogenesis
Major defects in vessel formation
MZ
CP
IZ
SVZ
VZ
MZ
CP
IZ
SVZ
VZ
X
Normal cortical development
Neuronal acellularity
Massive cortical degeneration

9

pothesis is supported by recent studies examining the role of the vasculature in neurogenesis in the adult rodent hippocampus and the higher vocal center (HVC) of the adult songbird neostriatum (Louissaint et al., 2002; Palmer, 2002; Palmer et al., 2000).

The heterozygous VEGF-A$^{nescre/+}$ mice show obvious changes in neuronal cellularity in the most superficial layers of the juvenile cortex. Interestingly, these layers of the cortex show the highest and most localized levels of cortical VEGF-A expression (Ogunshola et al., 2000), and we do observe specific defects in vascular patterning in this region. Given the above set of experiments, there may be altered neuronal migration into these layers or increased apoptosis as a result of changes in factors secreted from the altered microvascular environment. A summary model of the observed cortical defects observed in this study is presented in Fig. 9.

The autocrine role of VEGF-A/Flk1 in neurogenesis

Due to the severity of the neuronal degeneration observed in VEGF-A$^{nescre/hypo}$ mice, and the recent reports that VEGF-A may directly influence neuronal proliferation and differentiation decisions (Hobson et al., 2000; Jin et al., 2000, 2002; Ogunshola et al., 2002; Oosthuyse et al., 2001), we have investigated the potential autocrine role of Flk1 in vivo using a Cre recombinase-dependent *Flk1* conditional allele. Unlike the situation when we conditionally inactivated VEGF-A in the developing neuroectoderm, we have found no obvious phenotypes in mice lacking Flk1 in the developing nervous system. These results indicate that Flk1 does not play a direct, essential role in normal nervous system development. We cannot exclude the possibility that VEGF-A may still have direct effects on neuronal lineage development through the stimulation of other VEGF-A receptors (i.e., Flt1 and Neuropilin-1). Definitive genetic proof of the direct role of these receptors in VEGF-A signaling in neuronal development, however, awaits their nervous system-specific inactivation. With similar strategies to the one presented here, we expect that the putative, nonendothelial role of VEGF-A/Flk1 signaling can be addressed in other organ systems as well, such as in bone and retinal development (Robinson et al., 2001; Zelzer et al., 2002).

Acknowledgments

We thank Dr. Janet Rossant, Kristina Vintersten, and Marina Gertsenstein for the critical reading of this manuscript. J.H. is a recipient of a National Cancer Institute of Canada Research (NCIC) Fellowship. The study was also supported by the NCIC grant #21335 and the Novo Nordisk Foundation, the Swedish Cancer Foundation, IngaBritt and Arne Lundberg Foundation and Göteborg University (to C.B.). H.G. is supported by an EMBO postdoctoral fellowship and the Swedish Cancer Foundation. A.N. is a CIHR senior scientist.

References

Adams, R.H., Klein, R., 2000. Eph receptors and ephrin ligands: essential mediators of vascular development. Trends Cardiovasc. Med. 10, 183–188.

Banasiak, K.J., Xia, Y., Haddad, G.G., 2000. Mechanisms underlying hypoxia-induced neuronal apoptosis. Prog. Neurobiol. 62, 215–249.

Behrens, A., Haigh, J., Mechta-Grigoriou, F., Nagy, A., Yaniv, M., Wagner, E.F., 2003. Impaired intervertebral disc formation in the absence of Jun. Development 130, 103–109.

Breier, G., Albrecht, U., Sterrer, S., Risau, W., 1992. Expression of vascular endothelial growth factor during embryonic angiogenesis and endothelial cell differentiation. Development 114, 521–532.

Carmeliet, P., Collen, D., 1999. Role of vascular endothelial growth factor and vascular endothelial growth factor receptors in vascular development. Curr. Top. Microbiol. Immunol. 237, 133–158.

Carmeliet, P., Ferreira, V., Breier, G., Pollefeyt, S., Kieckens, L., Gertsenstein, M., Fahrig, M., Vandenhoeck, A., Harpal, K., Eberhardt, C., et al., 1996. Abnormal blood vessel development and lethality in embryos lacking a single VEGF allele. Nature 380, 435–439.

Carmeliet, P., Storkebaum, E., 2002. Vascular and neuronal effects of VEGF in the nervous system: implications for neurological disorders. Semin. Cell Dev. Biol. 13, 39–53.

Damert, A., Miquerol, L., Gertsenstein, M., Risau, W., Nagy, A., 2002. Insufficient VEGFA activity in yolk sac endoderm compromises haematopoietic and endothelial differentiation. Development 129, 1881–1892.

Dor, Y., Porat, R., Keshet, E., 2001. Vascular endothelial growth factor and vascular adjustments to perturbations in oxygen homeostasis. Am. J. Physiol. Cell Physiol. 280, C1367–C1374.

Dumont, D.J., Fong, G.H., Puri, M.C., Gradwohl, G., Alitalo, K., Breitman, M.L., 1995. Vascularization of the mouse embryo: a study of flk-1, tek, tie, and vascular endothelial growth factor expression during development. Dev. Dyn. 203, 80–92.

Ferrara, N., 2002. Role of vascular endothelial growth factor in physiologic and pathologic angiogenesis: therapeutic implications. Semin. Oncol. 29, 10–14.

Ferrara, N., Carver-Moore, K., Chen, H., Dowd, M., Lu, L., O'Shea, K.S., Powell-Braxton, L., Hillan, K.J., Moore, M.W., 1996. Heterozygous embryonic lethality induced by targeted inactivation of the VEGF gene. Nature 380, 439–442.

Fong, G.H., Rossant, J., Gertsenstein, M., Breitman, M.L., 1995. Role of the Flt-1 receptor tyrosine kinase in regulating the assembly of vascular endothelium. Nature 376, 66–70.

Gerber, H.P., Hillan, K.J., Ryan, A.M., Kowalski, J., Keller, G.A., Rangell, L., Wright, B.D., Radtke, F., Aguet, M., Ferrara, N., 1999. VEGF is

Fig. 8. Analysis of the forebrain of wild type (1st row, A–C) and Flk1$^{nescre/null}$ (2nd row, D–F) E13.5 embryos for cellularity (H&E staining, 1st column, A, D), apoptosis (TUNEL assay, 2nd column, B, E), and proliferation (Ki67 immunohistochemistry, 3rd column, C, F). Scale bars represent 50 μm.

Fig. 9. Summary model of observed cortical defects resulting from altered VEGF-A activity specifically in the developing nervous system. The defects fall into three sequentially connected categories: filopodium, vessel density, and cortical structure changes. Alterations in VEGF-A levels in the cortex lead to aberrations in filopodia development that translate into altered vessel branching and density. The abnormal vessel density leads to changes in the architecture of the cortex. The severity of the observed phenotypes is VEGF-A dosage-dependent. NF, neurotrophic factors; MZ, marginal zone; CP, cortical plate; IZ, intermediate zone; SVZ, subventricular zone; VZ, ventricular zone.

required for growth and survival in neonatal mice. Development 126, 1149–1159.
Haigh, J., McVeigh, J., Greer, P., 1996. The fps/fes tyrosine kinase is expressed in myeloid, vascular endothelial, epithelial, and neuronal cells and is localized in the trans-golgi network. Cell Growth Differ. 7, 931–944.
Hobson, M.I., Green, C.J., Terenghi, G., 2000. VEGF enhances intraneural angiogenesis and improves nerve regeneration after axotomy. J. Anat. 197 (Pt 4), 591–605.
Jin, K., Zhu, Y., Sun, Y., Mao, X.O., Xie, L., Greenberg, D.A., 2002. Vascular endothelial growth factor (VEGF) stimulates neurogenesis in vitro and in vivo. Proc. Natl. Acad. Sci. USA 99, 11946–11950.
Jin, K.L., Mao, X.O., Greenberg, D.A., 2000. Vascular endothelial growth factor: direct neuroprotective effect in in vitro ischemia. Proc. Natl. Acad. Sci. USA 97, 10242–10247.
Kawasaki, T., Kitsukawa, T., Bekku, Y., Matsuda, Y., Sanbo, M., Yagi, T., Fujisawa, H., 1999. A requirement for neuropilin-1 in embryonic vessel formation. Development 126, 4895–4902.
Kisanuki, Y.Y., Hammer, R.E., Miyazaki, J., Williams, S.C., Richardson, J.A., Yanagisawa, M., 2001. Tie2-Cre transgenic mice: a new model for endothelial cell-lineage analysis in vivo. Dev. Biol. 230, 230–242.
Kullander, K., Klein, R., 2002. Mechanisms and functions of Eph and ephrin signalling. Nat. Rev. Mol. Cell Biol. 3, 475–486.
Lee, Y.M., Jeong, C.H., Koo, S.Y., Son, M.J., Song, H.S., Bae, S.K., Raleigh, J.A., Chung, H.Y., Yoo, M.A., Kim, K.W., 2001. Determination of hypoxic region by hypoxia marker in developing mouse embryos in vivo: a possible signal for vessel development. Dev. Dyn. 220, 175–186.
Louissaint Jr., A., Rao, S., Leventhal, C., Goldman, S.A., 2002. Coordinated interaction of neurogenesis and angiogenesis in the adult songbird brain. Neuron 34, 945–960.
Lu, M., Adamis, A.P., 2002. Vascular endothelial growth factor gene regulation and action in diabetic retinopathy. Ophthalmol. Clin. North Am. 15, 69–79.
Matsuzaki, H., Tamatani, M., Yamaguchi, A., Namikawa, K., Kiyama, H., Vitek, M.P., Mitsuda, N., Tohyama, M., 2001. Vascular endothelial growth factor rescues hippocampal neurons from glutamate-induced toxicity: signal transduction cascades. FASEB J. 15, 1218–1220.
Millauer, B., Wizigmann-Voos, S., Schnurch, H., Martinez, R., Moller, N.P., Risau, W., Ullrich, A., 1993. High affinity VEGF binding and developmental expression suggest Flk-1 as a major regulator of vasculogenesis and angiogenesis. Cell 72, 835–846.
Miquerol, L., Gertsenstein, M., Harpal, K., Rossant, J., Nagy, A., 1999. Multiple developmental roles of VEGF suggested by a LacZ-tagged allele. Dev. Biol. 212, 307–322.
Muhlner, U., Mohle-Steinlein, U., Wizigmann-Voos, S., Christofori, G., Risau, W., Wagner, E.F., 1999. Formation of transformed endothelial cells in the absence of VEGFR-2/Flk-1 by Polyoma middle T oncogene. Oncogene 18, 4200–4210.
Neufeld, G., Cohen, T., Shraga, N., Lange, T., Kessler, O., Herzog, Y., 2002. The neuropilins: multifunctional semaphorin and VEGF receptors that modulate axon guidance and angiogenesis. Trends Cardiovasc. Med. 12, 13–19.
Ng, Y.S., Rohan, R., Sunday, M.E., Demello, D.E., D'Amore, P.A., 2001. Differential expression of VEGF isoforms in mouse during development and in the adult. Dev. Dyn. 220, 112–121.
Novak, A., Guo, C., Yang, W., Nagy, A., Lobe, C.G., 2000. Z/EG, a double reporter mouse line that expresses enhanced green fluorescent protein upon Cre-mediated excision. Genesis 28, 147–155.
Ogunshola, O.O., Antic, A., Donoghue, M.J., Fan, S.Y., Kim, H., Stewart, W.B., Madri, J.A., Ment, L.R., 2002. Paracrine and autocrine functions of neuronal vascular endothelial growth factor (VEGF) in the central nervous system. J. Biol. Chem. 277, 11410–11415.
Ogunshola, O.O., Stewart, W.B., Mihalcik, V., Solli, T., Madri, J.A., Ment, L.R., 2000. Neuronal VEGF expression correlates with angiogenesis in postnatal developing rat brain. Brain Res. Dev. Brain Res. 119, 139–153.
Oosthuyse, B., Moons, L., Storkebaum, E., Beck, H., Nuyens, D., Brusselmans, K., Van Dorpe, J., Hellings, P., Gorselink, M., Heymans, S., et al., 2001. Deletion of the hypoxia-response element in the vascular endothelial growth factor promoter causes motor neuron degeneration. Nat. Genet. 28, 131–138.
Orioli, D., Klein, R., 1997. The Eph receptor family: axonal guidance by contact repulsion. Trends Genet. 13, 354–359.
Palmer, T.D., 2002. Adult neurogenesis and the vascular Nietzsche. Neuron 34, 856–858.
Palmer, T.D., Willhoite, A.R., Gage, F.H., 2000. Vascular niche for adult hippocampal neurogenesis. J. Comp. Neurol. 425, 479–494.
Provis, J.M., Leech, J., Diaz, C.M., Penfold, P.L., Stone, J., Keshet, E., 1997. Development of the human retinal vasculature: cellular relations and VEGF expression. Exp. Eye Res. 65, 555–568.
Robinson, G.S., Ju, M., Shih, S.C., Xu, X., McMahon, G., Caldwell, R.B., Smith, L.E., 2001. Nonvascular role for VEGF: VEGFR-1, 2 activity is critical for neural retinal development. FASEB J. 15, 1215–1217.
Ruhrberg, C., Gerhardt, H., Golding, M., Watson, R., Ioannidou, S., Fujisawa, H., Betsholtz, C., Shima, D.T., 2002. Spatially restricted patterning cues provided by heparin-binding VEGF-A control blood vessel branching morphogenesis. Genes Dev. 16, 2684–2698.
Semenza, G.L., 2001. HIF-1 and mechanisms of hypoxia sensing. Curr. Opin. Cell Biol. 13, 167–171.
Shalaby, F., Rossant, J., Yamaguchi, T.P., Gertsenstein, M., Wu, X.F., Breitman, M.L., Schuh, A.C., 1995. Failure of blood-island formation and vasculogenesis in Flk-1-deficient mice. Nature 376, 62–66.
Shima, D.T., Mailhos, C., 2000. Vascular developmental biology: getting nervous. Curr. Opin. Genet. Dev. 10, 536–542.
Smith, L.E., 2002. Pathogenesis of retinopathy of prematurity. Acta Paediatr. Suppl. 91, 26–28.
Soker, S., Takashima, S., Miao, H.Q., Neufeld, G., Klagsbrun, M., 1998. Neuropilin-I is expressed by endothelial and tumor cells as an isoform-specific receptor for vascular endothelial growth factor. Cell 92, 735–745.
Sondell, M., Sundler, F., Kanje, M., 2000. Vascular endothelial growth factor is a neurotrophic factor which stimulates axonal outgrowth through the flk-1 receptor. Eur. J. Neurosci. 12, 4243–4254.
Stalmans, I., Ng, Y.S., Rohan, R., Fruttiger, M., Bouche, A., Yuce, A., Fujisawa, H., Hermans, B., Shani, M., Jansen, S., et al., 2002. Arteriolar and venular patterning in retinas of mice selectively expressing VEGF isoforms. J. Clin. Invest. 109, 327–336.
Tischer, E., Mitchell, R., Hartman, T., Silva, M., Gospodarowicz, D., Fiddes, J.C., Abraham, J.A., 1991. The human gene for vascular endothelial growth factor. Multiple protein forms are encoded through alternative exon splicing. J. Biol. Chem. 266, 11947–11954.
Tronche, F., Kellendonk, C., Kretz, O., Gass, P., Anlag, K., Orban, P.C., Bock, R., Klein, R., Schutz, G., 1999. Disruption of the glucocorticoid receptor gene in the nervous system results in reduced anxiety. Nat. Genet. 23, 99–103.
Varia, M.A., Calkins-Adams, D.P., Rinker, L.H., Kennedy, A.S., Novotny, D.B., Fowler Jr., W.C., Raleigh, J.A., 1998. Pimonidazole: a novel hypoxia marker for complementary study of tumor hypoxia and cell proliferation in cervical carcinoma. Gynecol. Oncol. 71, 270–277.
Zelzer, E., McLean, W., Ng, Y.S., Fukai, N., Reginato, A.M., Lovejoy, S., D'Amore, P.A., Olsen, B.R., 2002. Skeletal defects in VEGF(120/120) mice reveal multiple roles for VEGF in skeletogenesis. Development 129, 1893–1904.